Champagnac, J.-D., Schunegger, F., Norton, K., von Blanckenburg, F., Abbühl, L. M., Schwab, M. (2009): Erosion-driven uplift of the modern Central Alps. - Tectonophysics, 474, 1-2, 236-249

DOI: 10.1016/j.tecto.2009.02.024

Erosion-driven uplift of the modern Central Alps

Tectonophysics 2009

Jean-Daniel Champagnac (1)*, Fritz Schlunegger (2), Kevin Norton (1), Friedhelm von Blanckenburg (1,3), Luca M. Abbühl (2) and Marco Schwab (2)

1. Institut für Mineralogie, Universität Hannover, Callinstrasse 1, D-30167 Hannover, Germany.
2. Institute of Geological Sciences, University of Bern, Baltzerstrasse 1-3, CH-3012 Bern, Switzerland.
3. GeoForschungsZentrum Potsdam (GFZ), Telegrafenberg , D-14473 Potsdam, Germany.

*Corresponding author: Jean-Daniel Champagnac, Institut für Mineralogie, Universität Hannover, Callinstrasse 1, D-30167 Hannover. champagnac@gmail.com

Keywords: Passive unloading, sediment redistribution, isostatic rebound, Holocene deformation, rock uplift, lithosphere flexure.

Abstract

We present a compilation of data of modern tectono-geomorphic processes in the Central European Alps which suggest that observed rock uplift is a response to climate-driven denudation. This interpretation is predominantly based on the recent quantification of basin-averaged Late Holocene denudation rates that are so similar to the pattern and rates of rock uplift rates as determined by geodetic leveling. Furthermore, a GPS data-based synthesis of Adriatic microplate kinematics suggests that the Central Alps are currently not in a state of active convergence. Finally, we illustrate that the Central Alps have acted as a closed system for Holocene redistribution of sediment in which the peri-Alpine lakes have operated as a sink for the erosional products of the inner Central Alps.

While various hypotheses have been put forward to explain Central Alpine rock uplift (*e.g.* lithospheric forcing by convergence, mantle processes, or ice melting) we show with an elastic model of lithospheric deformation, that the correlation between erosion and rock uplift rates reflects a positive feedback between denudation and the associated isostatic response to unloading. Thus, erosion does not passively respond to advection of crustal material as might be the case in actively converging orogens. Rather, we suggest that the geomorphic response of the Alpine topography to glacial and fluvial erosion and the resulting disequilibrium for modern channelized and associated hillslope processes explains much of the pattern of modern denudation and hence rock uplift. Therefore, in a non-convergent orogen such as the Central European Alps, the observed vertical rock uplift is primarily a consequence of passive unloading due to erosion.

1. Introduction

Coupled models of lithospheric and surface processes have revealed the effects of feedback mechanisms between deep lithospheric and crustal processes leading to accretion of mass into the mountain belt, and surface erosion resulting in redistribution of mass from the orogen to the surrounding sedimentary basins (*e.g.* Dahlen et Suppe, 1988; Koons, 1989; Beaumont et al., 1992; Willett et al., 1993; Montgomery, 1994; Avouac and Burov, 1996; Burbank, 2002; Montgomery and Brandon, 2002; Hilley and Strecker, 2004; Whipple and Meade, 2004; 2006; Berger et al., 2008). The Central Alps (Fig. 1A) have served as a classical example to explore the geodynamic development of the coupled orogen/foreland basin system (*e.g.* Pfiffner, 1986; Schmid et al., 1996; Schlunegger et al., 2007), and to search for effects of possible feedback mechanisms between crustal accretion and surface erosion (Gilchrist et al., 1994; Schlunegger & Willett, 1999; Willett et al., 2006; Bonnet et al., 2007).

Geodetic levelling undertaken in the Central Alps (Schaer and Jeanrichard, 1974; Gubler et al., 1981; Kahle et al., 1997; Schlatter et al., 2005) initiated a series of work attempting to explain the pattern of modern rock uplift. These studies explore a whole range of geodynamic processes (or a combination of them), which potentially lead to the vertical motions. Active shortening between the Adriatic Promontory and the Eurasian Plate (Persaud and Pfiffner, 2004), often associated with mantle processes (Lyon-Caen and Molnar, 1989; Kuhlemann, 2007), melting of ice (Gudmundsson, 1994; Stocchi et al., 2005; Barletta et al. 2006), or erosion (Guillaume and Guillaume, 1981; Schlunegger & Hinderer, 2001; Cederbom et al., 2004) are invoked to explain the observed rock uplift. The finding that erosion rates are so similar to rock uplift rates let Wittmann et al (2007) to discuss possible causal relationships between uplift and erosion across temporal scales. Amongst these were: (i) coincidental agreement between erosion rates and rebound rates after ice melting; (ii) accretionary flux by active plate convergence being balanced by erosion; (iii) enhanced continuous Quaternary erosion and isostatic compensation of the mass removed .

The Holocene denudation rates from Wittmann et al. (2007), as well as the consideration of the importance of the mass balance associated with erosion (Champagnac et al., 2007) provide new constraints to quantitatively explore the hypothesis that rock uplift can be understood as flexural accommodation of the Alpine lithosphere to surface forcing. This paper explores whether modern rock uplift is a response to surface denudation, and thus to environmental effects. As evidence in of this view, we compiled five different sets of quantitative evidence. (i) Horizontal velocity data (GPS and seismotectonic) quantify the kinematics of the Adriatic Plate (Battaglia et al., 2004; Anderson and Jackson, 1987; Calais et al., 2002) and integrate plate motion over a decadal timescale. (ii) Geodetic levelling data calculated from centennial re-measurements of a first-order levelling line relative to a reference station north of the Alps yield information about vertical rock motion (Kahle et al, 1997; Schlatter et al., 2005). (iii) Sediment yields that are based on suspended loads of river sediment (Schlunegger & Hinderer, 2001; 2003; Schwab, 2007), integrate denudation over decadal time scales, and concentrations of cosmogenic nuclides in riverborn sand (Wittmann et al., 2007, Norton et al., 2008) integrate denudation over late Holocene time scales. (iv) Volumetric calculations of lake and valley fills yield information about the post Last Glacial Maximum (LGM) redistribution of mass from the Alps to neighboring sedimentary sinks (Hinderer, 2001). Finally, (v) morphometric observations from the Alpine topography are used here to assess the routing pattern of sediment, thereby allocating sediment sources and sinks since the termination of the LGM. These data are used as parameters of an elastic model of lithospheric bending in an effort to investigate how mass redistribution influences the flexure, and hence the magnitude of uplift of the Alps.

2. The Central Alps. Geologic setting and geomorphic evolution

2.1 Architecture and geodynamic evolution

The Central Alps (Fig. 1A) form a doubly-vergent orogen (Fig. 1B) with a crystalline core of European upper crust (Schmid et al., 1996). The Austroalpine sedimentary and crystalline nappes structurally overlie the (meta)sedimentary sequences of the Penninic and the Helvetic thrust nappes (Fig. 1B). North of these nappes lies the Molasse Basin, a sedimentary wedge made up of material derived from erosion of the rising Alps (*e.g.* Homewood et al., 1986). This basin is bordered to the north by the Jura fold-and-thrust belt. The southern side of the Central Alps comprises the Southern Alpine thrust sheets that consist of crystalline basement rocks and sedimentary units of Autro-alpine ("African") origin. This fold-and-thrust belt is bordered to the south by the upper Tertiary clastic deposits of the Po Basin. The modern tectonic architecture of the Central Alps (*e.g.* Schmid and Kissling, 2000) results from the continent-continent collision between the Adriatic and the European plates that started in the Late Cretaceous (*e.g.* Tricart, 1984; Schmid et al., 1996).

A major phase of lateral orogenic growth was initiated during the Lower and Middle Miocene with a shift of the active deformation fronts approximately 50 km farther south beneath the Po basin in the vicinity of Milano (Fantoni, 2001; Schönborn, 1992) and activation of the Jura thrusting that started sometime in the Late Miocene (Becker, 2000) and ceased prior to 3.4 Ma (Bolliger et al., 1993; Becker, 2000). This lateral growth increased the Alpine width from *ca.* 100 to 180 km (Schmid et al., 1996). A further major change in the geodynamic development occurred at the Mio-Pliocene boundary when rates of thrusting in the Southern Central Alps decreased, and when the Molasse Basin became uplifted and eroded (Willett et al., 2006; Cederbom et al., 2004). Also at the same time, deformation and exhumation became focused in the core of the Central Alps and particularly in the region surrounding the Aar massif (Pfiffner et al., 1997). Note, that Pliocene to modern deformation continued in the Jura Mountains at, however, very low horizontal displacement rates of approximately 0.05 mm/yr (Ustaszewski & Schmid, 2007). These slow rates of deformation are in agreement with the results of GPS surveys revealing relative movements between the Jura Mountains and the Eurasian Plate that are hardly different from zero (Walpersdorf et al., 2006). On the southern side of the Alps, compressive structures, loosely dated to the Pliocene and the Pleistocene, have been observed in the Po plain east of Lake Maggiore, with vertical displacement rates of 0.1-0.2 mm/yr (Sileo et al., 2007).

2.2 Paleo-climate and geomorphic evolution

A large worldwide Plio-Quaternary increase of terrigenous sediment yield has been proposed (Hay et al., 1988; Zhang et al., 2001; Molnar, 2004). Its origin seems to be related to global cooling (Zhang et al., 2001), changes in moisture pathways (Driscoll and Haug, 1998), and an increase in both magnitude and frequency of climate variability (Molnar, 2004). In the Alps, the consequence was a two- to threefold increase in sediment yields since 5-3 Ma as suggested by Kuhlemann et al. (2002). This increase was considered as evidence of a climatically-driven surface process change, a large component of which was attributed to increased precipitation (Cederbom et al., 2004) and erosion by glacial processes (Kuhlemann et al., 2001; Champagnac et al., 2007). The glacial erosion seems to have accelerated around 0.9 Ma as suggested by incision rates of a valley in the Central Alps (Häuselmann et al., 2007), and by information about vegetation and sedimentologic changes (Muttoni et al., 2003; Scardia et al., 2006).

The glacial overprint in the landscape is presumably the most important process setting the pace and pattern of modern surface erosion (*e.g.* Schlunegger & Hinderer, 2001). In particular, the morphometric properties of a glacial landscape, the changes in vegetation cover, and the high capacity of glaciers to remove sediments from the valleys create a landscape that is not in equilibrium with most modern fluvial and associated hillslope processes. Also, most of the large Alpine valleys currently operate as nearby sinks for sediment because the Alpine glaciers carved deep depressions where sediment started to accumulate after the retreat of the glaciers (Hinderer, 2001). This post-LGM storage of sediments (*e.g.* Lake Geneva, Lake Constance, and associated floodplains, Fig. 2A) presumably influenced the wavelength of rock uplift pattern via flexural accommodation. To conclude, it appears that the Pleistocene to present sediment production, transport and storage strongly depends on the glacial inheritance of the landscape.

3. Data sets of Holocene and modern surface processes

The information presented here is a combination between instrumental (GPS-based data, seismicity and terrestrial geodesy) hydrological and geochemical information (denudation), and geological (sedimentation) constraints. These data cover a range of time scales, which is potentially problematic. For example, GPS velocities, seismic moments, and geologic deformation may do not match because of deformation effects related to transients at all time scales (Friedrich et al. 2001). Therefore time extrapolation of GPS data has to be considered with care. The same potential pitfall concerns the comparison between geodetic data (uplift rates) and denudation rate data from cosmogenic nuclides. This could potentially provide a major uncertainty in our analysis that we cannot resolve at the moment.

3.1 Present-day kinematics

The present-day tectonics of the Central and Western Alps are mostly governed by the counter-clockwise rotation of the Adriatic Microplate relative to stable Europe (Nocquet and Calais, 2004). To better determine the Alpine kinematics, we used the three most comprehensive studies about the Adriatic microplate kinematics relative to stable Europe (Fig. 2A). Poles of rotation are located at [45.8N, 10.2E] based on focal mechanisms and energy release of earthquakes at the Adriatic microplate boundary (Anderson and Jackson, 1987), at [9.1E, 45.4N] using information from the permanent W-Alps GPS network REGAL (Calais et al., 2002), and at [8.1E ± 0.7, 46.3N±0.4] based on the GDAP Model that considers the European EUREF network and other data sources (Battaglia et al., 2004) and at [7.78E ± , 45.79N] based on 22 GPS sites in the Po Valley (D'Agostino et al., 2008). The average of these three rotation poles is [8.9E, 45.7N], located at the boundary between the Po Basin and the southern foothills of the Central Alps. This location of Adria’s Euler pole is consistent with the aseismicity of the Lepontine Dome (Delacou et al., 2004), the extensional and dextral seismotectonic regime in the Western Alps and in the Valais (Maurer et al., 1997, Deichmann et al., 2002), and with a compressional regime observed in seismotectonics and paleoseismology in the Eastern Alps, east of longitude 9.5°E (*e.g.* WORKING GROUP CPTI, 2004). It also explains the abundant occurrence of dextral strike-slip *vs.* the scarcity of sinistral strike-slip movements in the Western Alps (*e.g.,* Vialon et al., 1989; Collombet et al., 2002; Lickorish et al., 2002, Champagnac et al., 2004; Champagnac et al., 2006; Delacou et al., 2008). The counterclockwise rotation is inferred to be 0.52°/Ma (Calais et al., 2002), 0.9°±0.2°/Ma (Battaglia et al., 2004), and 0.309°± 0.022°/Ma with an average of 0.58°/Ma. Other calculations from Ward (1994) and Grenerczy et al. (2005) yielded slightly slower rotation rate of ~0.3°/Ma, but unrealistic Euler pole locations (from a tectonic viewpoint) farther to the northwest and to the west, respectively. In a synthesis of these and related studies, Nocquet and Calais. (2004) proposed that rotation of the Adriatic microplate implies NW-SE compression in the Eastern Alps, transitioning to dextral shear in the Central Alps, as well as transtensive deformation in the Western Alps.

3.2 Geodetic rock uplift

We used the geodetic data that has been repeatedly collected between *ca.* 1903 and 1990 and processed (Jeanrichard, 1975; Gubler et al., 1981; Kahle et al., 1997; Schlatter et al., 2005). These data are considered to reflect the velocity field of upper crustal levels, and we interpret these rates to reflect pattern of "rock uplift" (*sensu* England and Molnar, 1990, see also Stüwe and Barr, 1998 for a review of the terminology). We present a new polynomial (n=2) interpolation based on a database provided by A. Schlatter (Schlatter et al., 2005 and personal communication, 2007, Fig. 2C). This database corresponds to rates of near-surface rock uplift, since the artificial benchmarks have not been eroded during the decades of measurement. All vertical motions are relative to a specific benchmark near to the city of Aarburg, at the southern foothill of the Jura Mountains (Fig. 2). The relative rock uplift ranges from -0.4 mm/yr north of the Jura to 1.3 mm/yr within the core of the belt, and the isolines of rock uplift parallel the strike direction of the belt (N070º, Fig. 2C), with no relation to the Adriatic's Euler pole (see section 3.1).

The data infer that the Jura Mountains are subsiding with respect to the city of Aarburg (average of the ten most subsiding points equals -0.33 mm/yr). However, there is no geologic or geophysical evidence for subsidence. Rather, a series of Quaternary cut-terraces north of the Jura Mountains (Nivière and Winter, 2000), as well as very slow compressional neotectonic movements in this area (Ustaszewski & Schmid, 2007) suggest a small relative surface uplift. Therefore, the geodetic base level of Aarburg is very likely experiencing a positive vertical motion with respect to the undeformed reference lithosphere. As will be discussed later in this paper (section 3.4), the location of the geodetic base level also corresponds to the geomorphic base level for the sediment transfer system on the northern side of the Alps.

3.3 Denudation rates

3.3.1 Suspended loads

Present-day denudation rates are based on measurements of suspended sediment concentrations of the major Swiss rivers (Fig. 2B). The suspended loads have been regularly recorded by the Swiss Federal Hydrological Service over the last 20 to 30 years (Fig. 2B). The contribution of suspended sediment from tributary systems was subtracted to calculate the denudation rates for the headwaters of the trunk streams (Hinderer, 2001; Schlunegger and Hinderer, 2001, 2003; Schwab, 2007). A similar pattern of denudation rates, although with slightly different magnitudes, resulted from the 1993 survey. It is important to note here that the use of suspension load measurements over a short time period can often result in substantial underestimates of sediment transfer (*e.g.*, Kirchner et al., 2001; Schaller et al., 2001). Wittmann et al. (2007) observed such underestimates for the Central Alps by comparing river loads with cosmogenic nuclide-derived denudation rates (figs 2B and 2C). Underestimates possibly arose because of the lack of inclusion of solute and bedload transport, sediment trapping by retention dams, or because the time span during which suspended load concentrations have been measured is too short to sample the high-magnitude floods that are considered to be the most effective mechanisms for sediment discharge (Kirchner et al., 2001; Molnar, 2001; Dadson et al., 2003). Despite these drawbacks, the data show a consistent pattern that is characterized by an increase in denudation rates from <0.02 mm/yr in the foreland to >0.1 mm/yr in the Alpine core. Exceptionally high rates of 0.6 mm/yr are calculated for a tributary of the Rhine River in the eastern part of the Swiss Alps (Landquart River).

3.3.2. Denudation rates from cosmogenic ^{10}Be in river sediment

In a recent publication, Wittmann et al. (2007) applied in situ-produced cosmogenic nuclides to estimate erosion rates for various catchments in the Central Swiss Alps. This method, using the concentration of ^{10}Be in riverborn quartz (see von Blanckenburg, 2005, for a review of the method), includes the contribution of both physical and chemical denudation and provides spatially averaged denudation rates for the sampled watersheds. In the Alpine setting, this method integrates denudation over time scales of several hundreds to thousands of years (Wittmann et al., 2007). Terrestrial cosmogenic nuclides and the inferred pattern of denudation thus record the effects of high magnitude erosion events (von Blanckenburg, 2005). Accordingly, cosmogenic nuclides probably provide a more representative estimate of the late Holocene denudation rates than suspended loads of sediment. Denudation rates of catchments in the Central Alps increase from *ca.* 0.25 mm/yr in the Molasse Basin to more than 1 mm/yr in the core of the belt (1.28 mm/yr, Lonza River, Lötschental, Fig. 2C).

3.4 Post-LGM redistribution of sediment

An analysis of whether surface erosion has the capability to drive rock uplift must identify whether this sediment is actually removed from the system, or whether it is stored along the borders of the orogen, such that marginal loading of the lithosphere occurs. For example, the Rhine valley south of Lake Constance appears to act as a sediment sink which we can argue for with the following observation: the geodetic data imply differential uplift of approximately 1 mm/yr between Lake Constance and Chur (Figs. 2A and 2C). This implies that a step in base level of 10 m would have emerged between the two sites during Holocene. We would expect to see the formation of cut-terraces several meters high (Burbank & Anderson, 2001), which, however, is not the case. Indeed, the floodplain of the Rhine River is flat, and alluvial fans of locally sourced tributary systems display smooth transitions to the valley floor (Fig. 3A). These geomorphic features imply that the Rhine valley (including the Lake Constance), overdeepened during the glacial periods (Hinderer, 2001), has been (and still is) in the stage of sediment accumulation and has operated as a sedimentary sink, as do all perialpine lakes.

A topographic section across the Central Alps (Fig. 3B) supports the interpretation that the regions surrounding the Central Alps of Switzerland, and especially the large overdeepened valleys (*i.e.* the Rhone and Rhine valleys), and the (paleo)lakes in the Swiss Plateau have operated as sedimentary sinks since the retreat of the valley glaciers. Indeed, all large rivers with sources in the Central Alps (excluding the Po River) have been tributaries of at least one lake, usually with a large and flat floodplain immediately upstream of the lake. These lakes and floodplains have served to accumulate the erosional detritus from the core of the Central Alps. In other words, no sediments from the majority of the Central Alps (with the exception of the dissolved loads, and a small fraction of the suspended load) have left the belt since the termination of the Last Glacial Maximum. The situation is different in the Western Alps, where the paleo-lakes were filled before the Bølling (~ 12000 yr BP, Nicoud et al., 2002) and where sediment has been by-passed since then (*e.g.* Gresivaudan Lake, between Albertville and Grenoble).

Sediment export, however, does occur in the lower reaches of the Rhine River downstream of Lake Constance. Prominent knickzones in the longitudinal stream profile (*e.g.* the 23 m-high waterfall of the Rhine River) indicate the presence of an erosional front, shifting the signal of a lowered base level farther upstream (Figs. 4A and 4B). The effects of relative base level lowering are also seen by erosional fronts formed by tributaries of Rhine River in the Swiss Plateau. For instance, for the situation of the Aare River, the modern erosional front is currently located near Solothurn (Fig. 4C). Headward migration of these rivers has resulted in the formation of abandoned cut-terraces. These result from the difference in height between the local geomorphic base level of the Central Alps (the lakes of the Swiss Molasse Basin, at elevations between 370 and 550 m a.s.l.) and the lowered base level (the Upper Rhine Graben). Since the formation of knickzones requires differential vertical motion between distinct base levels (Burbank and Anderson, 2001), and because no sea level drop occurred during the late Holocene (*e.g.* Lambeck and Chappell, 2001), the occurrence of knickzones in the Swiss Plateau suggests that the local geomorphic base level (*i.e.* the northern portion of the Swiss Plateau including the reference station in Aarburg, Fig. 2) has experienced an upward vertical motion with respect to the undeformed reference lithosphere.

3.5 Relation between denudation and rock uplift

Wittmann et al. (2007) showed a close linkage between denudation rates and modern rock uplift rates. The pattern of denudation rates calculated from both ^{10}Be and suspended sediment load concentrations (see section 3.3.1 and 3.3.2, as well as Fig. 2B) is characterized by a trend of increasing rates from the Swiss Plateau to the core of the Central Alps. Furthermore, the catchments with highest denudation rates are also located in regions for which highest rock uplift rates of >1 mm/yr are currently measured (Fig. 2C).

In Figure 5 we show a statistical evaluation of the correlation first presented by Wittmann et al. (2007). For this purpose, mean rock uplift rates were calculated for the same catchments for which ^{10}Be data exist. The two sets of data are positively correlated, with a coefficient of correlation of 0.85. The best correlation between the data yields a slope of 0.88 ± 0.14 and a vertical axis (geodetic rock uplift) intercept of -0.03 ± 0.09 mm/yr (Fig. 5). This correlation and associated uncertainties have two important implications. First, the good correlation between uplift and denudation shows that both are tightly interlinked. The calculated slope of 0.88 suggests that rock uplift accounts roughly to 90% of denudation rate. This fact will be explored below with an elastic lithospheric model (section 4.3). Second, the zero vertical axis (geodetic rock uplift) intercept confirms the assumption made in section 3.2 that the geodetic base level is indeed identical to the geomorphic base level. In short, no erosion appears to occur where rates of rock uplift relative to base level is zero.

4. Controls on erosional unloading, and test of the isostatic rebound hypothesis

In the introduction, we briefly presented several hypotheses that have been put forward to explain the observed geodynamic data described along section 3. In this section we specifically test the hypothesis that the observed rock uplift is an isostatic response of the Alpine lithosphere to the mass transfer induced by erosion and deposition processes. We proceed by outlining in more details the hypothesis to be tested and by identifying the circumstances that have potentially controlled, and thus driven, the rates of orogen unloading. These information will be merged as input and boundary conditions for our model.

4.1 Erosional unloading

Since England (1981) and Guillaume and Guillaume (1982), different authors have claimed that the enhanced Plio-Quaternary erosion induced rock uplift in the Central and Western Alps *via* positive feedback mechanisms (Gilchrist et al., 1994; Schlunegger and Hinderer, 2001; 2003; Cederbom et al., 2004; Champagnac et al., 2007; Champagnac et al., 2008; van der Beek and Bourbon, 2008). In case where erosional unloading drives rock uplift through isostatic adjustment, the ratio between erosion and associated isostatic rebound is controlled by the density contrasts between the crust (ρ~2.8g/cm^3) and the mantle (ρ~3.25 g/cm^3). These density values have been suggested for the European Alps (*e.g.* Okaya et al., 1996; Viganò and Martin, 2007), yielding an isostatic response of ~5/6 (~80%) to erosional unloading. Therefore, a ratio between erosion and rock uplift rates close to 0.8 is expected for purely erosion-driven rock uplift in case of zero (or negligible) flexural rigidity. In the Central Alps, the rigidity is assumed to be small (T_e=5-20km, Steward and Watts, 1997), or even close to Airy conditions (Lyon-Caen and Molnar, 1989). The slope of the "rock uplift *vs.* denudation" relationship of the Central Alps (0.88 ± 0.14, Fig. 5) then provides support to the hypothesis that the rock uplift is simply a passive isostatic response to erosional unloading.

4.2 Environmental controls on erosional unloading

It has been shown that glacial and periglacial processes, coupled with changing fluvial erosion, are efficient drivers of erosion and sediment discharge (*e.g.* Church and Ryder, 1972 in Hinderer, 2001; Augustinus, 1992, 1995; Harbor, 1995; Hallet et al., 1996; Riihimaki et al., 2005; Herman and Braun, 2006). More specifically, the cyclic processes over a full glacial-interglacial interval, with glacier advances and retreats, variations in water runoff, changes in vegetation cover, and de-buttressing of unstable slopes enhance denudation in mountainous landscapes.

The transient state of the present-day Alpine topography was explored by Schlunegger & Hinderer (2003) who illustrated that the morphometry of the Alpine landscape still reflects to a large extent the overprint of the topography during the LGM. These authors suggested that glaciation affected the morphology of the Central Alps, with the modern topography dominated by glacial and periglacial features. This implies then that the morphometric and hypsometric properties of the Alpine landscape (*i.e.* steepness, concavity of hillslopes and channels, and hillslope-valley relationships) are not in equilibrium with the present-day situation (Brocklehurst and Whipple, 2004; Anderson et al., 2006; Korup & Schlunegger, 2008; Norton et al., 2008). As a result, modern fluvial and associated hillslope processes have resulted in the formation of V-shaped scars in landscapes that were formerly shaped by glacial processes, which is a strong evidence for ongoing re-adjustment of the Alpine topography to modern conditions (Fig. 6). As a consequence, surface erosion, denudation rates and sediment discharge are controlled by the extent to which glacial processes shaped the Alps during the LGM, even if glacial erosion is not the prime cause of high denudation rates. In support of this hypothesis Schlunegger & Hinderer (2001) revealed a positive correlation between present-day sediment yields and rock volumes excavated by glacial processes (see also Robl et al. [2008], for a related study in the Eastern Alps). We interpret therefore, that sediment yield has been enhanced in drainage basins with strong glacial overprint. Hence, the modern denudation would be driven by the present-day transient state of the Alpine landscape.

4.3 Isostatic response to erosional unloading

We numerically explored the spatial distribution of rock uplift and subsidence as controlled by (1) Late Holocene denudation from the core of the belt, (2) recent sedimentation to the adjacent Alpine valleys and (3) post LGM sedimentation in peri-Alpine lakes. In all cases, flexural rigidity, as well as other rheological parameters were constant and uniform, and the loading (or unloading) matrix was introduced into a simple two-dimensional flexural model, with instantaneous response to the loading (Watts, 2001, eq. 3.53). Different values for the elastic thickness (Te = 10-20 km, e.g. Royden, 1993; Steward and Watts, 1997) and Young's Modulus ($E = 7*10^{10} - 1*10^{11}$ [Turcotte & Schubert, 1982; Petrini and Podlachkov, 2000; Burov and Watts, 2006]) were tested. A Poisson's ratio of 0.25 (Christensen,1996) and a crustal density of 2.8 g/cm3 were kept constant. Edge effects were controlled by artificially extending the boundaries of the model by 100 km beyond the margins of the mountain belt in every direction. Like all elastic models, this model is a simple stress balance, and is not time-dependent. Also, it assumes states of isostatic equilibrium before loading and/or unloading. Thus, results are presented in unit of length (m), and directly converted into rates (mm/yr) for legibility of comparisons (Fig 7), assuming an instantaneous reaction at a constant rate.

Denudation data were projected on a cross-section, and the polynomial best fits (n=3) were calculated (Fig. 7A). The orientation of the projection line (N150º) was optimized in order to maximize the R^2 of the interpolation (R^2 max = 0.83). It is perpendicular to the Alpine trend (Fig. 7C). A value of 0 mm/yr was assigned to a point near Aarburg which represents the geomorphic base level, for both rock uplift and denudation (see section 3.5 for justification). Calculations of isostatically driven rock uplift induced by erosional unloading (Champagnac et al., 2007) are based on the interpolated values. In order to take into account the 2D flexural response to the lithosphere, the cross section was cylindrically expanded into 3D.

Figure 7A presents the rock uplift resulting from isostatic response to the fitted denudation pattern using an elastic thickness of 10 km and a Young's modulus of $1*10^{11}$ (rigidity = $8.9 * 10^{21}$ N.m, dashed line). The calculated maximal vertical velocity is located in the core of the belt and is in the order of +0.8 mm/yr with respect to Aarburg,. We can compare this result to the actual observed rock uplift (red dots, Fig. 7D). The model results are shown by the long-dashed line; they fit 75% of the observations. However, the predicted values are systematically higher than the observed values in the foreland basin (+0.2 mm/yr), whereas they are systematically lower in the southern flank of the belt (-0.2 mm/yr). Calculations of a more realistic scenario, including sediment trapping in the lakes are presented below.

As explored in section 3.4, the presence of lakes and paleo-lakes around the Central Alps during a relatively short time after deglaciation implies a more complex mass redistribution than if the products of erosion were simply removed from the system as assumed in the previous model (Champagnac et al., 2007 and above). Therefore, the effect of the loading due to sedimentation in the lakes was calculated for both the present and the situation immediately following the LGM (~20ka, Ivy-Ochs et al., 2004). Because sediments with a density of 2.5 g/cm^3 replace water with a density of 1g/cm^3, a relative density of 1.5 g/cm^3 was used for lake infills (Hinderer, 2001). Because of the spatial distribution of the lakes these calculations were done in map view. For the present-day situation, the load matrix entered in the model was built using the present-day location of the lakes and averaged sedimentation rate of 1762 mm/kyr (Hinderer, 2001). For the post-LGM calculation, the sedimentation area (paleo-lakes) was defined as the present lakes and the flat valleys upstream (defined as slopes of <0.5º), and the sedimentation rate as the average over the post-LGM and the Holocene (5122 mm/kyr, Hinderer, 2001). In both cases, the potential (and unknown) sediment loading in the Po Basin, the Upper Rhine Graben or the Bresse Graben was not introduced in our calculations.

The resulting effects of present-day lake loading are shown in Figure 7B. The lithospheric flexure due to sediment loading appears to be significant only around the larger lakes, and remains smaller than -0.1 mm/yr (max. value of 0.09 mm/yr for Lake Geneva, Te=10 km, Fig. 7B). In the swath cross-section used for unloading calculations (Fig. 7C), the loading effect of sedimentation in the rather small lakes is less than -0.03 mm/yr, and hence negligible. Over the post-LGM time scale, the effect of the loading is more important. The subsidence associated with sediment loading appears to be higher in large lakes (Geneva and Constance, up to -0.4 mm/yr), and a significant bending of the lithosphere up to -0.2 mm/yr is observed in the Swiss Plateau (Fig. 7C and blue line on Fig. 7D). In cross-section, a simple addition of the flexures calculated for erosional (Fig. 7A) and sedimentation processes (Fig. 7C and blue line Fig. 7D) yields a pattern of vertical movements that fits better the observed rock uplift at the northern flank of the belt (short-dashed line, Fig. 7D). The systematic over-prediction of 0.2 mm/yr of rock uplift calculated with the erosion model (see above) in the foreland basin is dramatically reduced when the post-LGM loading is taken into account.

Overall, adding the effect of lake loading results in minor deviations from the pure erosion unloading model (section 4.3.2). This is mainly due to the lower relative density of sediments and the size of the lakes, which is small with respect to the typical flexural wavelength of the Alpine lithosphere. Nevertheless, it appears that the consideration of sediment loading in the foreland basin allows the model to better predict observations of a tight curvature of rock uplift increase, especially at the northern side of the belt (Fig. 7D).

5. Discussion of alternative processes driving rock uplift

5.1 Modern crustal convergence

The ongoing convergence between the Adriatic microplate and Europe has often been called upon to explain the observed pattern of rock uplift (*e.g.* Persaud and Pfiffner, 2004, Lardaux et al., 2006) modulated by surface erosion (Schlunegger & Hinderer, 2001). It was shown above that the present-day location of the Adriatic microplate pole of rotation (at the limit of the Central Alps and the Po plain, close to [8.9E, 45.7N], see section 2.3 and Fig. 2A) is inside (or very close to) the plate itself, and induces rotational behavior of the plate at a debated rate ranging from 0.3°/Ma to 0.9°/Ma (see references in section 3.1). Note that our point here is not to discard local neotectonic evidence of shortening observed in the Central and Western Alps, but to explore the ability of plate convergence to drive the observed rock uplift. We can address this test by posing the question of the convergence rate that would be required to create the observed rock uplift. We can infer the required convergence rate by an orogen-scale mass balance by a reverse model approach. To this end we equated the orogenic flux with the erosional flux over the width of the orogen which contains the implicit assumption that rock uplift rate equals erosion rate. Then

$$V= (U*W)/D$$

with U being the mean observed rock uplift (U=0.6mm/yr, see section 3.2), W the width of the orogen (W=150km, see Fig 1) and D the mean depth of the accreted uppercrustal mass (D= 15 km, Mosar, 1999, Fig. 1). We thus can determine that the convergence rate across the Central Alps that would fully explain the observed rock uplift would be of the order of 6mm/yr. This value can be compared with the maximum potential rock uplift induced by the shortening determined by GPS across the Central Alps. A rate of 0.9°/Ma of counterclockwise rotation applied on a deformed area with a 100km-long radius (including the uncertainties on the Euler pole location, see Figure 2A) implies a shortening rate of ~1.6 mm/yr across the belt at the easternmost end of our study area. This maximum value of shortening, associated with the same geometric values than above (mid-crustal detachment at depth of 15 km and orogen's width of 150km) yields a tectonic flux of ~23.5m^2/yr and thus the maximum rock uplift induced by crustal accretion would be 0.16 mm/yr integrated over the entire cross section. This is much less than the observed rock uplift. More realistic kinematic values, including the fact that the study area is located to the western side of the ellipse error of the Euler pole location, yield much lower shortening rates across the belt (less than 1 mm/yr). Hence (<0.2 mm/yr) tectonically induced rock uplift in a large part of the Central Alps is negligible.

Note also that the pattern of rock uplift rate is spatially disconnected to the location of the rotation pole, and rock uplift also occurs in the Western Alps (Stocchi et al., 2005), where large-scale extension was clearly documented (Sue et al., 2000; Calais et al., 2002; Delacou et al., 2004; Champagnac et al., 2006). Therefore, the large discrepancy between the rate of shortening derived from the reversed model and the rate invoked from kinematic data either imply that the GPS data do not reflect ongoing (and hypothetical) long-term shortening, or that horizontal plate kinematics cannot be the main agent of rock uplift in the Central and Western Alps.

5.2 Ice melting.

Gudmundsson (1994) interpreted the pattern of modern rock uplift in terms of a visco-elastic rebound of the crust after removal of the glacial loads at the end of the LGM. This interpretation for the present-day rock uplift, however, implies a good knowledge of rheologic parameters (viscosity) to determine the time-dependent evolution of the rebound. Moreover, based on considerations of the reconstruction of LGM ice surface geometry of Florineth and Schlüchter (1998, 2000), Persaud & Pfiffner (2004) argued that a post-glacial rebound is not capable to explain the asymmetrical pattern of rock uplift as this pattern does not mimic the spatial ice loading. Instead, rock uplift was suggested to control the long-term denudation rate pattern deduced from apatite fission track ages, hinting at a long-term rock uplift control over denudation (Persaud & Pfiffner, 2004).

On the basis of a thorough ice cap and sea level change mass balance, Stocchi et al. (2005) concluded that the rock uplift associated with LGM ice melting range from -0.25 mm/yr to +0.25 mm/yr depending on the specifics of the applied ice model. For a shorter time scale, Barletta et al. (2006) showed that the post Little Ice Age (post 1850 A.D.) and ongoing glacier shrinkage plays an important role (20% to 50%) in the present-day rock uplift. They claim, however, that the drainage geometry and surface erosion potentially affect locations and rates of highest rock uplift. It is important to keep in mind that a potential rebound associated with ice melting is only a transient state towards a state of equilibrium. The finite deformation and exhumation over a succession of many glacial-interglacial periods is insensitive to this process (Champagnac et al., 2008). The rate of exhumation rates over million of years (fission track ages, Vernon et al., 2008) is of the same order of magnitude as those of the Late Holocene (~1 mm/yr or 1 km/Ma) and the thermal history reflects the average of short term denudation variations.

Finally, Wittmann et al. (2007) have questioned how denudation would agree with rock uplift if the time scales for rock uplift were short. For increased rock uplift to result in increased denudation rates, extensive migration of knickpoints and propagation of the erosional front into the entire landscape are required. This is, however, not the case as revealed by various regional studies (e.g., Schlunegger & Schneider, 2005; Korup & Schlunegger, 2008). Wittmann and co-authors considered it unlikely that such an adjustment can have taken place in a period as short as 15 ka, not to mention the few hundred years since the Little Ice Age. Therefore, although no consensus has been reached on the effect of ice melting on vertical movement of the Alpine lithosphere, no study has unambiguously demonstrated that melting-induced rebound has actually played a major role as a driving force of the observed rock uplift.

5.3 Mantle dynamics

The crust of the Central and Western Alps is between 40 to 60 km thick as inferred from depth determinations of the Moho (Waldhauser et al., 1998; Touvenod et al., 2007; Lombardi et al., 2008). A full isostatic compensation of such a thick crustal root would imply a mean elevation between ~1500m and ~3700m (Airy hypothesis). These values are higher than the observed mean elevations in the Alps (up to 2500 m calculated over a 30 km radius). This discrepancy is particularly obvious in the Lepontine Dome (the southern part of our transect, see Fig. 2D), where the mean altitude is less than 1500 m, despite a crustal thickness of 50-55 km. Therefore, either the large-scale relief is in a transient state, and is currently evolving to reach a new equilibrium at higher elevations, or a dense continental lithosphere beneath the Western and Central Alps contributes to maintain a gravitational equilibrium. In fact, teleseismic tomography images of the Alpine lithosphere show a complex structure, interpreted as partially delaminated lithosphere beneath the Western and Central Alps (Lippitch et al. 2003; Kissling, personal communication 2007). Lippitsch et al. (2003) interpreted this feature as a "slab tearing" from south to north (from under the Western Alps and toward the Central Alps). As demonstrated by numerical models (Gemmer and Houseman, 2007; Göğüs and Pysklywec, 2008), lithospheric gravitational instabilities potentially induce both rock uplift and subsidence, and may be applied to the Central Alps. Based only on gravity anomalies, Lyon-Caen & Molnar (1989) reached a similar conclusion, and found that recent rapid uplift of the Alps might be the result of the removal of a downward force that maintained the chain in a state of overcompensation. In the Central Alps, a contribution of processes operating at the interface between mantle and lower crust has to be invoked to explain the rock uplift pattern at the southern side of the belt, where denudation exceeds rock uplift. It might also explain the occurrence of uplift of the Swiss Plateau relative to the undeformed reference lithosphere on the northern side of the Alpine belt, seen by headward erosion of the Rhine River and the formation of the prominent waterfall. Hence, deep-seated processes could provide an explanation for a large wavelength component of uplift. However, they cannot explain the small-scale variations of rock uplift and particularly the tight curvature of uplift isolines next to the northern border of the Central Alps (Fig. 2C).

6. Implications and conclusions

Based on our data compilation, we tested whether modern rock uplift in the Alps may be the consequence of passive unloading due to erosion using a simple elastic model. The model results show that the lithospheric bending associated with this mass redistribution explains most of the rock uplift observed in the northern flank of the belt. The model predictions agree well with observations when temporary storage of sediment in the peri-Alpine lakes are taken into account. However, the numerical model only explains ~70% of the observed rock uplift to the southern side of the belt (Lepontine area), where rock uplift actually exceeds denudation (Fig. 7D). The unloading due to the melting of an ice body mostly located in large valleys over the entire belt (*e.g.* Florineth and Schlüchter (2000) is unlikely to produce the rock uplift in excess observed in the southern side of the Central Alps. Furthermore, the very slow active convergence across the Central Alps also fails to explain the excess of rock uplift there. Geophysical data show that the continental lithosphere is being delaminated under the Western Alps, and not (yet ?) under the Central Alps. The Holocene excess of rock uplift to the southern flank of the belt may be a direct evidence of the current operation of this process.

This study, based on accurate rate data, shows that a mountain belt can live and be actively eroded after the discontinuation of convergence. Rock uplift driven by erosional unloading will be active as long as a crustal root is present, with a decrease of the mean relief at 1/6 of the denudation rate (several tens of Ma at the present rate).

Acknowledgements

This work was supported by the Swiss NSF grant # PA002-117441 (JDC) and 119785 (FS), and DFG grant BL562-2 (FvB). Andreas Schlatter, Bundesamt für Landestopographie Switzerland is aknowledged for supplying rock uplift data. Robert S. Anderson is aknowledged for sharing his elastic code. We warmly thank Kurt Stüwe and Onno Oncken for insightful reviews, as well as the associate editor (Sierd Cloetingh) and an anonymous reviewer on an earlier version of the manuscript.

References

Anderson, R.S., Molnar, P. and Kessler, M.A., 2006. Features of glacial valley profiles simply explained. Journal of the Geophysical Research F: Earth Surface 111, doi:10.1029/2005JF000344.

Anderson, H. and Jackson, J., 1987. Active tectonics in the Adriatic region. Geophysical Journal Royal Astronomical Society 91, 937–983.

Augustinus, P.C., 1992. The influence of rock mass strength on glacial valley cross-profile morphometry, a case study from the Southern Alps, New Zealand. Earth Surface Processes and Landforms 17, 39-51.

Augustinus, P.C., 1995. Glacial valley cross-profile development: the influence of in situ rock stress and rock mass strength, with examples from the Southern Alps, New Zealand. Geomorphology 14, 87-97.

Avouac, J.P. and Burov, E.B., 1996. Erosion as a driving mechanism of intracontinental mountain growth. Journal of Geophysical Research B: Solid Earth 101, 17747-17769.

Barletta, V.R., Ferrari, C., Diolaiuti, G., Carnielli, T., Sabadini, R. and Smiraglia, C., 2006. Glacier shrinkage and modeled uplift of the Alps. Geophysical Research Letters 33, L14307, doi:10.1029/2006GL026490.

Battaglia, M., Murray, M.H., Serpelloni, E. and Burgmann, R., 2004. The Adriatic region: An independent microplate within the Africa-Eurasia collision zone. Geophysical Research Letter 31, L09605, doi:10.1029/2004GL019723.

Beaumont, C., Fullsack, P. and Hamilton, J., 1992. Erosional control of active compressional orogens, *in* Clay, M.C., ed., Thrust Tectonics: New York, Chapman and Hall, p. 1-31.

Becker, A. The Jura Mountains - an active foreland fold-and-thrust belt? Tectonophysics 321, 381–406.

Berger, A.L., Gulick, S.P., Spotila, J.A., Upton, P., Jaeger, J.M., Chapman, J.B., Worthington, L.A., Pavlis, T.L., Ridgeway, K.D., Willem, B.A., and McAlleer, R.J., 2008. Quaternary tectonic response to intensified glacial erosion in an orogenic wedge, Nature Geosciences 1, 793-799, doi:10.1038/ngeo334.

Bolliger, T., Engesser, B. and Weidmann, M., 1993. Première découverte des mammifères pliocènes dans le Jura neuchâtelois. Eclogae geologicae Helvetiae 86(3), 1031–1068.

Bonnet C., Malavieille, J. and Mosar, J., 2007. Interactions between tectonics, erosion, and sedimentation during the recent evolution of the Alpine orogen: Analogue modeling insights, Tectonics, 26, TC6016, doi:10.1029/2006TC002048.

Brocklehurst, S.H. and Whipple, K.X., 2004. Hypsometry of glaciated landscape. Earth Surface Processes and Landforms 29, 907-926, DOI: 10.1002/esp.1083.

Burbank, D.W., 2002. Rates of erosion and their implications for exhumation. Mineralogical Magazine, 66 (1), 25-52.

Burbank, D.W. and Anderson, R.S., 2001. Tectonic geomorphology. Blackwell Scientific, Oxford, 274 pp.

Burov, E.B. and Watts, A.B., 2006. The long-term strength of continental lithosphere: “jelly sandwich” or “crème brûlée”? GSA Today 16, 4-10, DOI: 10.1130/1052-5173(2006)016<4:TLTSOC>2.0.CO;2.

Calais, E., Nocquet, J., Jouanne, F. and Tardy, M., 2002. Current strain regime in the Western Alps from continuous Global Positioning System measurements, 1996 – 2001. Geology 30, 651-654.

Cederbom, C.E., Sinclair, H.D., Schlunegger, F., and Rahn, M.K., 2004. Climate-induced rebound and exhumation of the European Alps, Geology, 32 (8), pp. 709-712, doi: 10.1130/G20491.1.

Champagnac, J.-D., Sue, C., Delacou, B., and Burkhard, M., 2004.Brittle deformation in the inner NW Alps: From early orogen-parallel extrusion to late orogen-perpendicular collapse. Terra Nova 16(4),232-242, doi: 10.1111/j.1365-3121.2004.00555.x.

Champagnac, J.-D., Sue, C., Delacou, B., Tricart, P., Allanic, C. and Burkhard, M., 2006. Miocene lateral extrusion in the inner western Alps revealed by dynamic fault analysis. Tectonics 25 (3), doi:10.1029/2004TC001779.

Champagnac, J.-D., Molnar, P., Anderson, R.S., Sue, C. and Delacou, B., 2007. Quaternary erosion-induced isostatic rebound in the western Alps. Geology 35, 195-198, doi: 10.1130/G23053A.1.

Champagnac, J.-D., Van Der Beek, P., Diraison, G. and Dauphin, S., 2008. Flexural isostatic response of the Alps to increased Quaternary erosion recorded by foreland basin remnants, SE France. Terra Nova, 20 (3), 213-220, doi: 10.1111/j.1365-3121.2008.00809.x.

Church M. and Ryder J., 1972. Paraglacial sedimentation: a consideration of fluvial processes conditioned by glaciation. Bulletin of the Geological Society of America 83, 3059–3071.

Collombet, M., Thomas, J.C., Chauvin, A., Tricart, P., Bouillin, J.P. and Gratier, J.P., 2002. Counterclockwise rotation of the western Alps since the Oligocene: New insights from paleomagnetic data. Tectonics 21 (4), 14-1.

Christensen, N.I., 1996. Poisson's ratio and crustal seismology (1996) Journal of Geophysical Research B: Solid Earth, 101(2), 3139-3156.

Dadson, S.J., Hovius, N., Chen, H., Dade, W.B., Hsieh, M.L., Willett, S.D., Hu, J.C., Horng, M.J., Chen, M.C., Stark, C.P., Lague, D. and Lin, J.C., 2003. Links between erosion, runoff variability and seismicity in the Taiwan Orogen. Nature 426, 648-651.

Dahlen, F.A. and Suppe, J., 1988. Mechanics, growth, and erosion of mountain belts, *in* Clark, S.P., Burchfiel, B.C., and Suppe, J., eds., Processes in Continental Lithospheric Deformation. Geological Society of America Volume Special 218, 161-178.

Deichmann, N., Baer, M., Braunmiller, J., Ballarin Dolfin, D., Bay, F., Bernardi, F., Delouis, B., Faeh, D., Gerstenberger, M., Giardini, D., Huber, S., Kradolfer, U., Maraini, S., Oprsal, I., Schibler, R., Schler, T., Sellami, S., Steimen, S., Wiemer, S., Woessner, J. and Wyss, A., 2002. Earthquakes in Switzerland and surrounding regions during 2001. Eclogae Geologicae Helvetiae 95(2)2, 249-261.

Delacou, B., Sue, C., Champagnac, J.-D. and Burkhard, M., 2004. Present-day geodynamics in the bend of the western and central Alps as constrained by earthquake analysis. Geophysical Journal International 158 (2), 753-774, doi: 10.1111/j.1365-246X.2004.02320.x.

Delacou, B., Sue, C., Nocquet, J.-M., Champagnac, J.-D., Allanic, C., and Burkhard, M., 2008. Quantification of strain rate in the Western Alps using geodesy: Comparisons with seismotectonics. Swiss Journal of Geosciences 101 (2), 377-385, DOI 10.1007/s00015-008-1271-3.

Driscoll, N.W. and Haug, G.H., 1998. A Short Circuit in Thermohaline Circulation: A Cause for Northern Hemisphere Glaciation? Science 282, 436-438.

England, P., 1981. Metamorphic pressure estimates and sediment volumes for the Alpine orogeny: an independent control on geobarometers? Earth and Planetary Science Letters, 56, 387-397.

England, P. and Molnar, P., 1990. Surface uplift, uplift of rocks, and exhumation of rocks. Geology 18 (12), 1173-1177.

Fantoni, R., Massari, F., Minervini, M., Rogledi, S. and Rossi, M., 2001. Il Messiniano del margine Sudalpino-Padano: relazioni tra contesto strutturale e stratigrafico-deposizionale. Geologica Insubrica 6, 95–108.

Florineth, D. and Schlüchter, C., 1998. Reconstructing the Last Glacial Maximum (LGM) ice surface geometry and flowlines in the Central Swiss Alps. Eclogae Geologicae Helvetiae 91, 391– 407.

Florineth, D. and Schlüchter, C., 2000. Alpine evidence for atmospheric circulation patterns in Europe during the last glacial maximum. Quaternary Research 54, 295–308.

Friedrich, A.M., Lee, J., Wernicke, B.P., and Sieh, K., 2001. Geologic context of geodetic data across a Basin and Range normal fault, Crescent Valley, Nevada. Tectonics 23, TC2015, doi:10.1029/2003TC001528

Gilchrist, A.R., Summerfield, M.A. and Cockburn, H.A.P., 1994.Landscape dissection, isostatic uplift, and the morphologic development of orogens. Geology 22, 963-966.

Gemmer, L. and Houseman, G.A., 2007. Convergence and extension driven by lithospheric gravitational instability: evolution of the Alpine–Carpathian–Pannonian system. Geophysical Journal International 168, 1276-1290 doi: 10.1111/j.1365-246X.2006.03327.x.

Göğüs, O., and Pysklywec1, R., 2008 Near-surface diagnostics of dripping or delaminating lithosphere, Journal of Geophysical Research B: Solid Earth 113, doi:10.1029/2007JB005123

Grasso, A. and Jakob, A., 2003. Charge de sédiments en suspension: comparaison entre deux méthodes de calcul. Gaz Eaux Eaux usées (GWA) 82, 898-905.

Grenerczy, G., Sella, G., Stein, S. and Kenyeres, A., 2005. Tectonic implications of the GPS velocity field in the northern Adriatic region. Geophysical Research Letters 32 (16), L16311, 1-4.

Gubler, E., Kahle, H.-G., Klingelé, E., Mueller, S and Olivier, R., 1981. Recent crustal movements in Switzerland and their geophysical interpretation. Tectonophysics 71, 125-152.

Gudmundsson, G., 1994. An order-of-magnitude estimate of the current uplift-rates in Switzerland caused by the Wurm Alpine deglaciation. Eclogae Geologicae Helvetiae 87, 545-557.

Guillaume, A. and Guillaume, S., 1982. L'érosion dans les Alpes au Plio-Quaternaire et au Miocène. Eclogae Geologicae Helvetiae, 75, 247-268.

Hallet, B., Hunter, L. and Bogen, J., 1996. Rates of erosion and sediment evacuation by glaciers: A review of field data and their implications. Global and Planetary Change 12, 213-235, doi:10.1016/0921-8181(95)00021-6.

Harbor, J.M., 1995. Development of glacial-valley cross sections under conditions of spatially variable resistance to erosion. In: J.M. Harbor (ed.), «Glacial Geomorphology: Process and Form Development». Geomorphology 14, 99-107.

Häuselmann, P., Granger, D.E., Jeannin, P.Y. and Lauritzen, S.E., 2007. Abrupt glacial valley incision at 0.8 Ma dated from cave deposits in Switzerland. Geology 35, 143-146.

Hay, W.W., Sloan, J.L. and Wold, C.N., 1988. Mass/age distribution and composition of sediments on the ocean floor and the global rate of sediment subduction. Journal of Geophysical Research-B: Solid Earth 93, 14933-14940.

Herman, F. and Braun, J., 2006. Fluvial response to horizontal shortening and glaciations: A study in the Southern Alps of New Zealand. Journal of Geophysical Research-F: Earth Surface 111, doi:10.1029/2004JF000248.

Hilley, G.E. and Strecker, M.R, 2004. Steady state erosion of critical Coulomb wedges with applications to Taiwan and the Himalaya. Journal of Geophysical Research-B: Solid Earth 109, B01411, doi:10.1029/2002JB002284.

Hinderer, M., 2001. Late Quaternary denudation of the Alps, valley and lake fillings and modern river loads. Geodinamica Acta 14, 231-263.

Homewood, P., Allen, P.A., and Williams, G.D., 1986. Dynamics of the Molasse Basin of western Switzerland. Foreland basins, pp. 199-217.

Ivy-Ochs, S., Schäfer, J., Kubik, P.W., Synal, H.-A. and Schlüchter, C., 2004. Timing of deglaciation on the northern Alpine foreland (Switzerland). Eclogae Geologicae Helvetiae 97(1), 47-55, DOI: 10.1007/s00015-004-1110-0.

Jeanrichard, F., 1972. summary of geodetic studies of recent crustal movements in Switzerland. Tectonophysics 29, 289-292.

Kahle, H.G., Geiger, A., Bürki, B., Gubler, E., Marti, U., Wirth, B., Rothacher, M., Gurtner, W., Beutler, G., Bauersima, I. and Pfiffner, O.A., 1997. Recent crustal movements, geoid and density distribution: contribution from integrated satellite and terrestrial measurements. In: Pfiffner, O.A., Lehner, P., Heitzmann, P., Müller, St., Steck, A. (Eds.): Results of the National Research Program 20 (NRP 20). Birkhäuser, Basel, pp. 251-259.

Kirchner, J., Finkel, R., Riebe, C., Granger, D., Clayton, J., King, J. and Megahan, W., 2001. Mountain erosion over 10 yr, 10 k.y., and 10 m.y. time scales. Geology 29, 591-594.

Koons, P.O., 1989. The topographic evolution of collisional mountain belts: A numerical look at the Southern Alps of New Zealand. American Journal of Sciences 289, 1041-1069.

Korup, O. and Schlunegger, F., 2007. Bedrock landsliding, river incision, and transience of geomorphic hillslope-channel coupling: evidence from inner gorges in the Swiss Alps. Journal of Geophysical Research F: Earth Surface 12 (3), F03027.

Kuhlemann, J., 2007. Paleogeographic and paleotopographic evolution of the Swiss and Eastern Alps since the Oligocene. Global and Planetary Change 58(1-4), pp. 224-236, doi:10.1016/j.gloplacha.2007.03.007.

Kuhlemann, J., Frisch, W., Dunkl, I. and Szekely, B., 2001. Quantifying tectonic versus erosive denudation by the sediment budget; the Miocene core complexes of the Alps. Tectonophysics 330, 1-23.

Kuhlemann, J., Frisch, W., Szekely, B., Dunkl, I. and Kazmer, M., 2002. Postcollisional sediment budget history of the Alps: Tectonic versus climatic control. International Journal of Earth Sciences, 91, 818–837, doi: 10.1007/s00531-002-0266-y.

Lambeck, K. and Chappell, J., 2001. Sea Level Change Through the Last Glacial Cycle. Science 292, 679-686.

Lardeaux, J.M., Schwartz, S., Tricart, P., Paul, A., Guillot, S., Béthoux, N. and Masson, F. 2006. A crustal-scale cross-section of the south-western Alps combining geophysical and geological imagery. Terra Nova 18 (6), 412-422.

Lickorish, W.H., Ford, M., Burgisser, J. and Cobbold, P.R., 2002. Arcuate thrust systems in sandbox experiments: A comparison to the external arcs of the Western Alps. Bulletin of the Geological Society of America 114 (9), 1089-1107.

Lippitsch, R., Kissling, E. and Ansorge, J., 2003. Upper mantle structure beneath the Alpine orogen from high-resolution teleseismic tomography. Journal of Geophysical Research-B-Solid Earth 108(B8), doi:10.1029/2002JB002016.

Lombardi, D., Braunmiller, J., Kissling, E. and Giardini, G., 2008. Moho depth and Poisson's ratio in the Western–Central Alps from receiver functions. Geophysical Journal International 173, 249–264 doi: 10.1111/j.1365-246X.2007.03706.x.

Lyon-Caen, H. and Molnar, P., 1989. Constraints on the deep structure and dynamic processes beneath the Alps and adjacent regions from an analysis of gravity anomalies. Geophysical Journal International 99, 19-32.

Maurer, H., Burkhard, M., Deichmann, N. and Green, G., 1997. Active tectonism in the central Alps: contrasting stress regimes north and south of the Rhone Valley. Terra Nova 9, 91–94.

Molnar, P., 2001. Climate change, flooding in arid environments, and erosion rates. Geology 29, 1071–1074.

Molnar, P., 2004. Late Cenozoic increase in accumulation rates of terrestrial sediment: How might climate change have affected erosion rates ? Annual Review of Earth and Planetary Sciences 32, 67–89, doi: 10.1146/annurev.earth.32.091003.143456.

Mosar, J., 1999. Present-day and future tectonic underplating in the western Swiss Alps: reconciliation of basement wrench-faulting and decollement folding of the Jura and Molasse basin in the Alpine foreland. Earth and Planetary Science Letters 173, 143–155.

Montgomery, D.R., 1994. Valley incision and the uplift of mountain peak. Journal of Geophysical Research, B: Solid Earth 99, 13913-13921.

Montgomery, D.R. and Brandon, M.T., 2002. Topographic controls on erosion rates in tectonically active mountain ranges. Earth and Planetary Science Letters. 201, 481-489.

Muttoni, G., Carcano, C., Garzanti, E., Ghielmi, M., Piccin, A., Pini, R., Rogledi, S. and Sciunnach, D., 2003. Onset of major Pleistocene glaciations in the Alps. Geology 31, 989-992.

Nicoud, G., Royer, G., Corbin, J.-C., Lemeille, F. and Paillet, A., 2002. Creusement et remplissage de la vallée de l'Isère au Quaternaire récent. Apports nouveaux du forage GMB1 (1999) dans la région de Grenoble (France). Glacial erosion and infilling of the Isère valley during the recent Quaternary. New results from borehole GMB1 in the Grenoble area (France). Géologie de la France 4, 39-49.

Nivière, B. and Winter, T., 2000. Pleistocene northwards fold propagation of the Jura within the southern Upper Rhine graben: Seismotectonic implications. Global and Planetary Change 27 (1-4), 263-288.

Nocquet, J.-M., and Calais, E., 2004. Geodetic Measurements of Crustal Deformation in the Western Mediterranean and Europe. Pure and applied geophysic 161, doi DOI 10.1007/s00024-003-2468-z.

Norton, K.P., von Blanckenburg, F., Schlunegger, F., Schwab, M. and Kubik, P.W., 2008. Cosmogenic nuclide-based investigation of spatial erosion and hillslope channel coupling in the transient foreland of the Swiss Alps. Geomorphology, 95, 474–486.

Okaya, N., Cloetingh, S., and Mueller, S., 1996. A lithospheric cross-section through the Swiss Alps - II. Constraints on the mechanical structure of a continent-continent collision zone. Geophysical Journal International, 127(2), pp. 399-414.

Persaud, M. and Pfiffner, O.A., 2004. Active deformation in the eastern Swiss Alps: post-glacial faults, seismicity and surface uplift. Tectonophysics 385, 59-84.

Petrini, K. and Podlachkov, Y., 2000. Lithospheric pressure–depth relationship in compressive regions of thickened crust. Journal of metamorphic Geology 18, 67–77.

Pfiffner, O.A., 1986. Evolution of the north Alpine foreland basin in the central Alps. In: Allen, P.A., Homewood, P. (Eds.): Foreland basins. International Association of Sedimentologists Special Publication 8, 219-228.

Pfiffner, O.A., Sahli, S. and Stäuble, M., 1997. Structure and evolution of the external basement uplifts (Aar, Aiguilles Rouges/Mt. Blanc). In: Pfiffner, O.A., Lehner, P., Heitzmann, P., Müller, St., Steck, A. (Eds.): Results of the National Research Program 20 (NRP 20).Birkhäuser, Basel, pp. 139-153.

Pfiffner, O.A., Schlunegger F. and Buiter, S., 2002. The Swiss Alps and their peripheral foreland basin: stratigraphic response to deep crustal processes. Tectonics 21, 3.1-3.16.

Riihimaki, C.A., MacGregor, K.R., Anderson, R.S., Anderson, S.P. and Loso, M.G., 2005. Sediment evacuation and glacial erosion rates at a small alpine glacier. Journal of Geophysical Research 110. doi:10.1029/2004JF000189.

Robl, J., Hergarten, S., Stüwe, K., 2008. Morphological analysis of the drainage system in the Eastern Alps. Tectonophysics 460 (1–4), 263–277. doi:10.1016/j.tecto.2008.08.024.

Royden, L.H., 1993. The tectonic expression slab pull at continental convergent boundaries. Tectonics 12(2), 303-325.

Scardia, G., Muttoni, G., and Sciunnach, D., 2006. Subsurface magnetostratigraphy of Pleistocene sediments from the Po Plain (Italy): Constraints on rates of sedimentation and rock uplift. Bulletin of the Geological Society of America 118(11-12), 1299-1312.

Schaer, J.P., and Jeanrichard, F., 1974. Mouvements verticaux anciens et actuels dans les Alpes suisses. Eclogae Geologicae Helvetiae, 67(1), 101-119.

Schaller, M., von Blanckenburg, F., Hovius, N. and Kubik, P.W., 2001. Large-scale erosion rates from in situ-produced cosmogenic nuclides in European river sediments. Earth and Planetary Science Letters 188, 441-458, doi:10.1016/S0012-821X(01)00320-X .

Schlatter, A., Schneider, D., Geiger, A. and Kahle, H.-G., 2005. Recent vertical movements from precise levelling in the vicinity of the city of Basel, Switzerland. International Journal of Earth Sciences 94 (4), 507-514, DOI: 10.1007/s00531-004-0449-9.

Schlunegger, F. and Willett, S.D., 1999. Spatial and temporal variations in exhumation of the Central Swiss Alps and implications for exhumation mechanisms. In: Brandon, M., Willett, S.D. (Eds.): Exhumation processes: normal faulting, ductile flow, and erosion. Geological Society of London Special Publication 154, 157-180.

Schlunegger, F. and Hinderer, M., 2001. Crustal uplift in the Alps: Why the drainage pattern matters. Terra Nova, 13, 425-432.

Schlunegger, F. and Hinderer, M. 2003: Pleistocene/Holocene climate change, re-establishment of fluvial drainage network and increase in relief in the Swiss Alps. Terra Nova 15, 88-95.

Schlunegger, F. & Schneider, H. 2005: Pleistocene/Holocene climate change, relief-rejuvenation and topographic length scales in a fluvial drainage basin, Napf area, Central Switzerland. Geomorphology 69, 102-117.

Schlunegger, F., Rieke-Zapp, D. and Ramseyer, K., 2007. Possible environmental effects on the evolution of the Alps-Molasse Basin system. Swiss Journal of Geosciences 3, 383-406.

Schmid, S.M., Pfiffner, O.A., Froitzheim, N., Schönborn, G. and Kissling, E., 1996. Geophysical-geological transect and tectonic evolution of the Swiss-Italian Alps. Tectonics 15, 1036-1064.

Schmid, S.M. and Kissling, E., 2000. The arc of the Western Alps in the light of geophysical data on deep crustal structure. Tectonics 19, 62-85.

Schönborn, G., 1992. Alpine tectonics and kinematic models of the central Southern Alps. Memorie di Scienze Geologiche (Padova) 44, 229-393.

Schwab, M., 2007. Identification and controls of sediment sources in the Swiss Alps; case studies in Entlebuch (Lucerne) and Lumnezia (Graubünden). Unpublished PhD thesis, university of Bern, 107 pp.

Schlatter, A., Schneider, D., Geiger, A. and Kahle, H.-G., 2005. Recent vertical movements from precise levelling in the vicinity of the city of Basel, Switzerland. International Journal of Earth Sciences 94(4), 507-514, DOI10.1007/s00531-004-0449-9.

Sileo, G., Giardina, F., Livio, F., Michetti, A.M., Mueller, K., and Vittori, E., 2007. Remarks on the Quaternary tectonics of the Insubria Region (Lombardia, NW Italy, and Ticino, SE Switzerland). Bollettino della Societa Geologica Italiana 126(2), 411-425.

Spreafico, M., Lehmann, C., Jakob, A. and Grasso, A., 2005. Feststoffbeobachtungen in der Schweiz – Ein Tätigkeitsbereicht der Landeshydrologie. Nr. 8, Bundesamt für Wasser und Geologie, Bern, 99 pp.

Stewart, J. and Watts, A.B., 1997. Gravity anomalies and spatial variations of flexural rigidity at mountain ranges. Journal of Geophysical Research B: Solid Earth, 102 (B3), 5327-5352.

Stocchi, P., Spada, G. and Cianetti, S., 2005. Isostatic rebound following the Alpine deglaciation: impact on the sea level variations and vertical movements in the Mediterranean region. Geophysical Journal International 162, 137-147, doi: 10.1111/j.1365-246X.2005.02653.x.

Stüwe, K. and Barr, T.D., 1998. On uplift and exhumation during convergence. Tectonics 17(1), 80-88.

Sue, C., Martinod, J., Tricart, P., Thouvenot, F., Gamond, J.-F., Frechet, J., Marinier, D., Glot, J.-P. and Grasso, J.-R., 2000. Active deformation in the inner western Alps inferred from comparison between 1972-classical and 1996-GPS geodetic surveys. Tectonophysics 320, 17-29.

Thouvenot, F., Paul, A., Fréchet, J., Béthoux, N., Jenatton, L., and Guiguet, R.. 2007. Are there really superposed Mohos in the southwestern Alps? New seismic data from fan-profiling reflections. Geophysical Journal International 170(3), 1180-1194, doi: 10.1111/j.1365-246X.2007.03463.x

Tricart, P., 1984. From passive margin to continental collision: A tectonic scenario for the Western Alps, American Journal of Science 284, 97-120.

Turcotte, D.L. and Schubert, G., 1982. Geodynamics: Application of continuum physics to geological problems. John Wiley, New York, 650 pp.

Ustaszewski, K and Schmid, S., 2007. Latest Pliocene to recent thick-skinned tectonics at the Upper Rhine Graben-Jura Mountains junction. Swiss Journal of Geosciences 100, 293-312.

van der Beek, P. and Bourbon, P., 2008. A quantification of the glacial imprint on relief development in the French western Alps. Geomorphology 97, 52–72. doi:10.1016/j.geomorph.2007.02.038.

Vialon, P., Rochette, P. and Ménard, G., 1989. Indentation and rotation in the western alpine arc. In: Coward, M.P., Dietrich, D., Park, R.G. (Eds.), Alpine Tectonics. Geological Society of London Special Publication 45, 329-338.

Vernon, A.J., van der Beek, P.A., Sinclair, H.D., and Rahn, M.K, 2008. Increase in late Neogene denudation of the European Alps confirmed by isoage analysis of a fission-track database. Earth and Planetary Science Letters 270 (3-4), 316-329,DOI : 10.1016/j.epsl.2008.03.053

von Blanckenburg, F., 2005. The control mechanisms of erosion and weathering at basin scale from cosmogenic nuclides in river sediment. Earth and Planetary Science Letters 237, 462-479.

Viganò, A. and Martin, S., 2007. Thermorheological model for the European Central Alps: brittle–ductile transition and lithospheric strength. Terra Nova 19, 309-316, doi: 10.1111/j.1365-3121.2007.00751.x

Waldhauser, F., Kissling, E., Ansorge, J., and Mueller, S., 1998. Three-dimensional interface modelling with two-dimensional seismic data: the Alpine crust-mantle boundary. Geophysical Journal International 135, 264–278, doi:10.1046/j.1365-246X.1998.00647.x.

Walpersdorf, A., Baize, S., Calais, E., Tregoning, P., and Mocquet, J.-M., 2006. Deformation in the Jura Mountains (France): First results from semi-permanent GPS measurements. Deformation in the Jura Mountains (France): First results from semi-permanent GPS measurements. Earth and Planetary Science Letters 245, 365–372.

Ward, S.N., 1994. Constraints on the seismotectonics of the central Mediterranean from very long baseline interferometry. Geophysical Journal International 117,441–452.

Watts, A.B., 2001. Isostasy and flexure of the lithosphere. Cambridge university Press, 458 p.

Willett, S., Beaumont, C., and Fullsack, P., 1993. Mechanical model for the tectonics of doubly vergent compressional orogens. Geology 21, 371-374.

Willett, S.,D., Schlunegger, F., and Picotti, V., 2006. Messinian climate change and erosional destruction of the central European Alps. Geology 34, 613-616.

Whipple, K.X. and Meade, B.J., 2004. Controls on the strength of coupling among climate, erosion, and deformation in two-sided, frictional orogenic wedges at steady state. Journal of Geophysical Research-Earth Surface 109, doi:10.1029/2003JF000019.

Whipple, K.X. and Meade, B.J., 2006. Orogen response to changes in climatic and tectonic forcing. Earth and Planetary Science Letters 243, (1-2), 218-228.

Wittmann, H., von Blanckenburg, F., Kruesmann, T., Norton, K.P., and Kubik, P., 2007. The relation between rock uplift and denudation from cosmogenic nuclides in river sediment in the Central Alps of Switzerland. Journal of Geophysical Research-Earth Surface 112, doi:10.1029/2006JF000729.

WORKING GROUP CPTI (2004) - *Catalogo Parametrico Terremoti Italiani, version 2004.* INGV, Bologna. http://emidius.mi.ingv.it/CPTI/.

Zhang, P., Molnar, P., and Downs, W.R., 2001. Increased sedimentation rates and grain sizes 2-4 Myr ago due to the influence of climate change on erosion rates. Nature 410, 891-897.

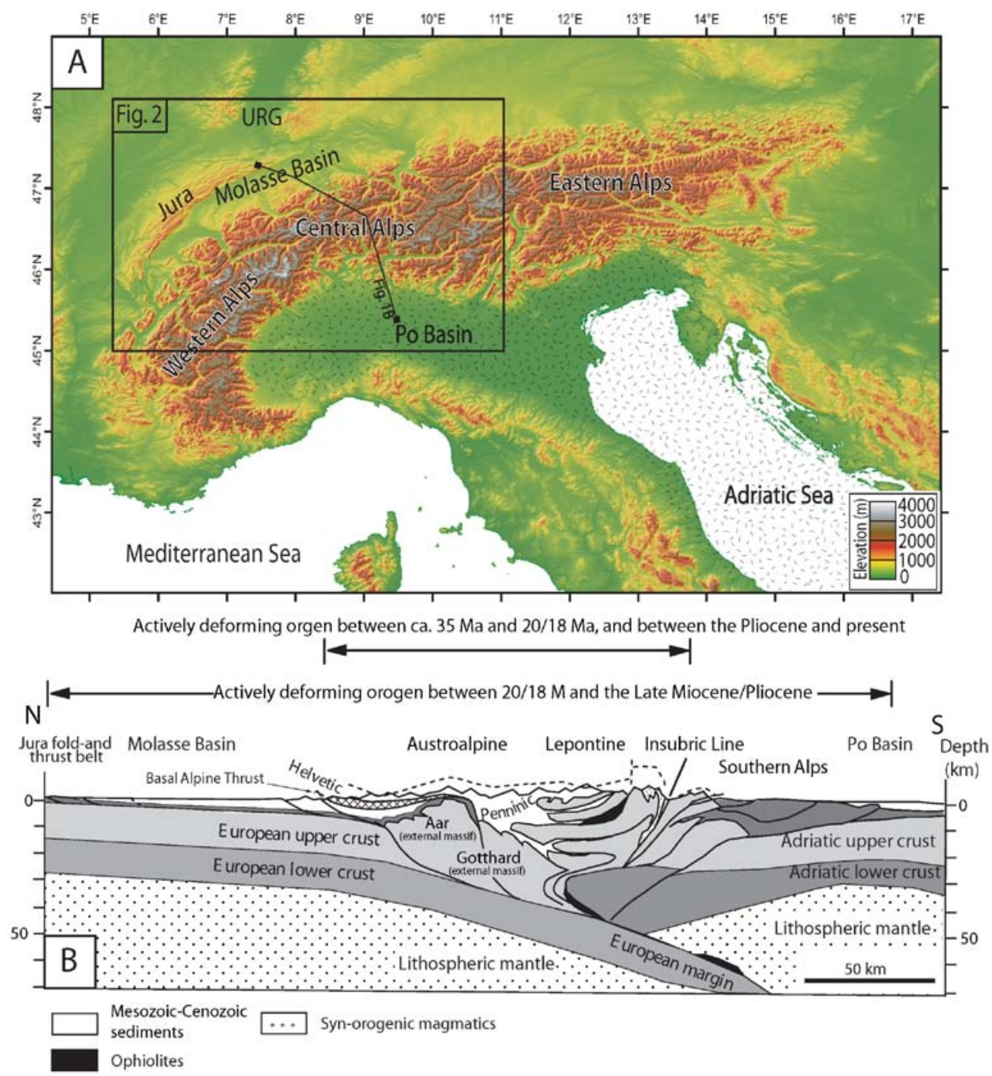

Fig. 1: (A) Topography of the Alps including major thrust systems. IL: Insubric Line, URG: Upper Rhine Graben. The thick line corresponds to the cross section shown in Figure 1B. The Adriatic Microplate is symbolized by dashed area.

(B) Cross section of Central Alps showing major tectonic units, as well as the change of deformation width through time. Modified after Pfiffner et al. (2002).

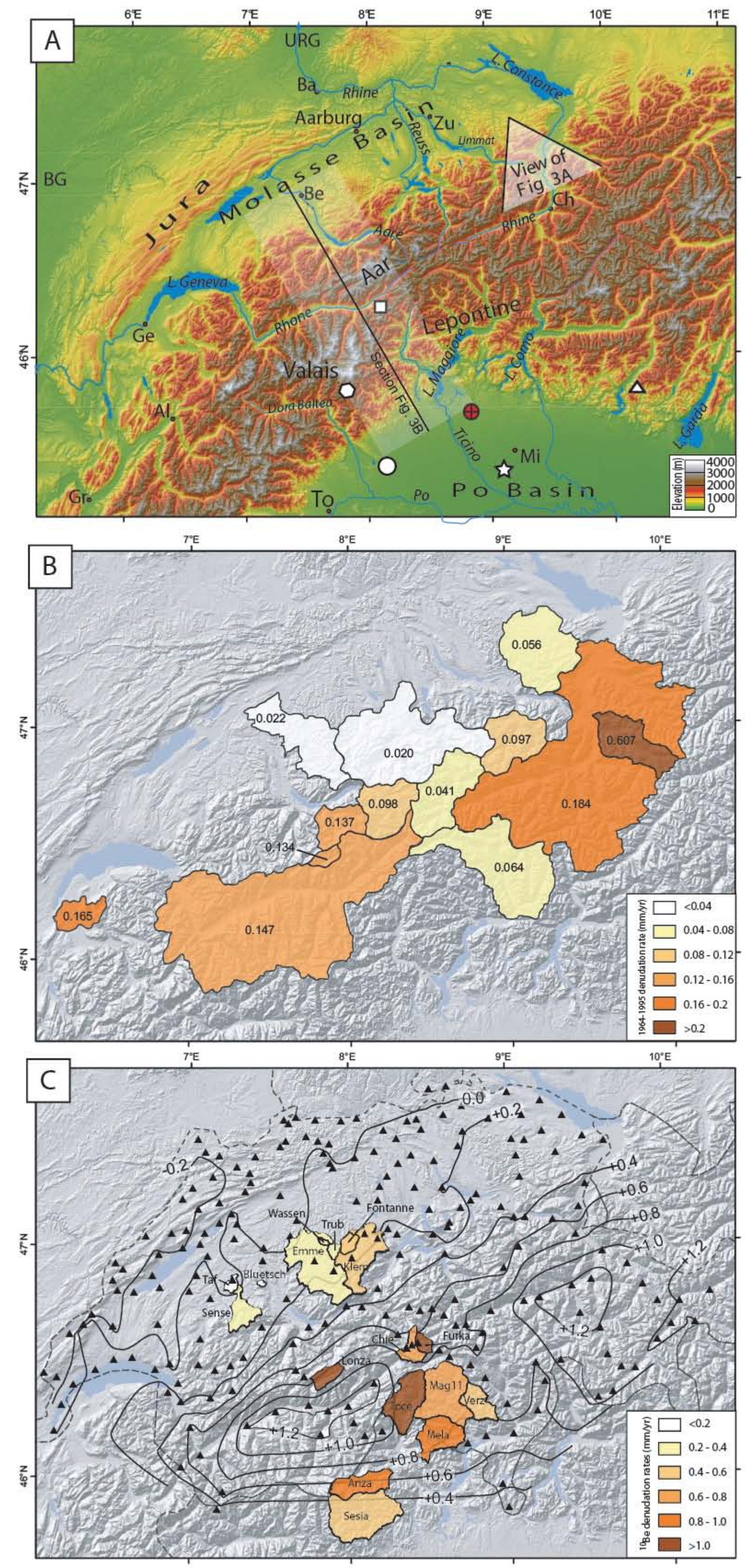
A
B
C
URG
Ba
Rhine
Aarburg
Zu
Reuss
Limmat
L. Constance
View of Fig 3A
Jura
Molasse Basin
BG
Be
Ch
Aare
Aar
L. Geneva
Rhone
Lepontine
Ge
Valais
Section Fig. 3B
L. Maggiore
L. Como
Dora Baltea
Al
Ticino
Mi
To
Po
Po Basin
Gr
L. Garda
Elevation (m)
1964-1995 denudation rate (mm/yr)
<0.04
0.04 - 0.08
0.08 - 0.12
0.12 - 0.16
0.16 - 0.2
>0.2
Wassen
Trub
Fontanne
Emme
Ilfis
Taf
Bluetsch
Sense
Chie
Furka
Lonza
Mag11
Verz
Mela
Anza
Sesia
^{10}Be denudation rates (mm/yr)
<0.2
0.2 - 0.4
0.4 - 0.6
0.6 - 0.8
0.8 - 1.0
>1.0

Fig. 2: (A) Topography of the Central Alps including illustration of the largest rivers and lakes. Also shown are the positions of the Euler poles of the Adriatic microplate (square, Battaglia et al., 2004; star, Calais et al., 2002; triangle, Anderson and Jackson, 1987; red circle, average of these five rotation points). Al: Albertville, Be: Bern, Ge: Geneva, Gr: Grenoble, Mi: Milano, To, Torino, Zh: Zürich, Ch: Chur, Ba: Basel, URG: Upper Rhine Graben, BG: Bresse Graben. The transparent bar indicates the section along which minimum and maximum elevations were extracted for the topographic analysis (see Fig. 3B), as well as the projection line for denudation data (see Fig. 6).

(B) Denudation rates that are based on suspended loads of sediment. The denudation rates were originally calculated by Schlunegger and Hinderer (2001, 2003), and subsequently modified by Spreafico et al. (2005) and Schwab (2007) using the duration curve method of Grasso and Jakob (2003).

(C) Contour of the watersheds sampled for cosmogenic 10Be-derived denudation rates from Wittmann et al. (2007), with the Trub and Fontanne catchments added from Norton et al. (2008). Only samples from trunk streams have been used, and replicates have been averaged. The results of moraine and periglacial samples (Wittmann et al., 2007) are discarded here because they do not represent steady-state denudation nuclide concentrations. Curved lines represent equal rock uplift with respect to the city of Aarburg, Kahle et al., 1997; Schlatter et al., 2005. Geodetic measurement locations are shown as black triangles.

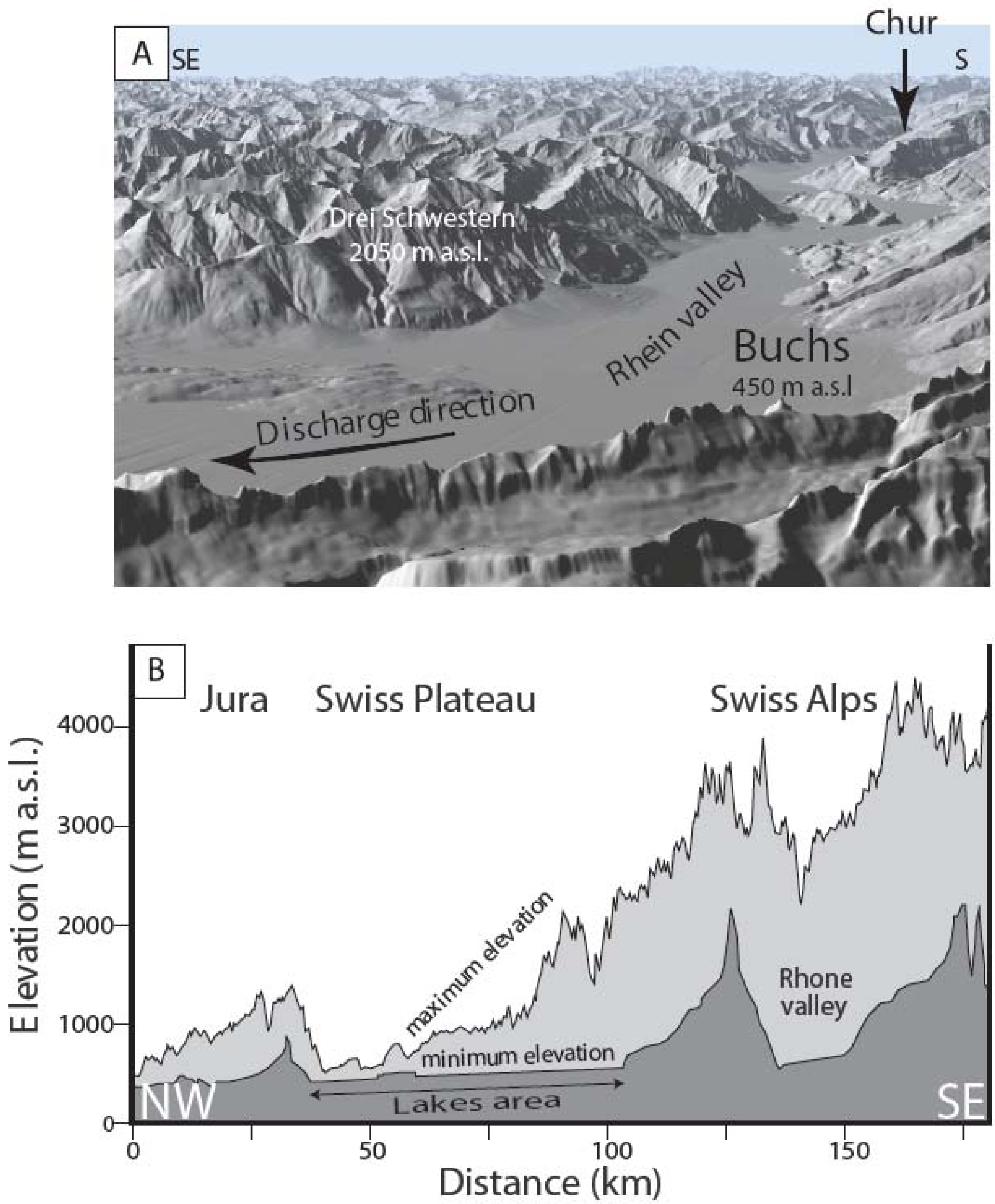

Fig. 3: (A) Perspective view of the Rhine valley towards Chur; note the absence of cut terraces.

(B) Minimum and maximum elevations that are extracted from a 25 m DEM within a 25-km-wide swath profile as shown in Fig. 2a. The flat ramp of the foreland valley serves as potential sediment trap.

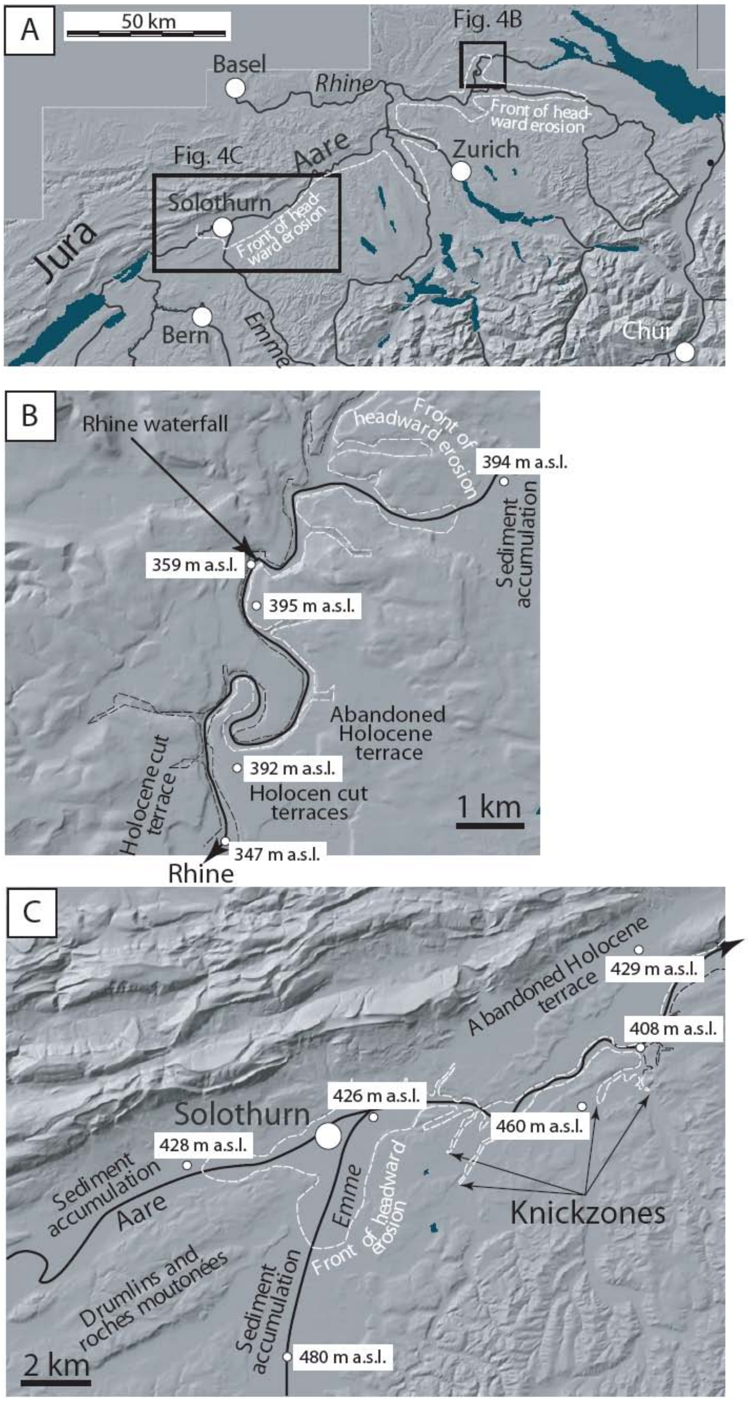

Fig. 4: (A) Topography of the Swiss Alps including delineation of front of headward erosion (presence of knickpoints) in the north.

(B) Confluence between the Emme and the Aare Rivers in the Molasse Basin. Note the presence of cut terraces that form in response to headward erosion, indicating migration of the erosional front in the upstream direction, and sediment accumulation upstream of these knickpoints (see text for details)

(C) Illustration of the topographic situation near Lake Constance at the outlet of the Rhine river.

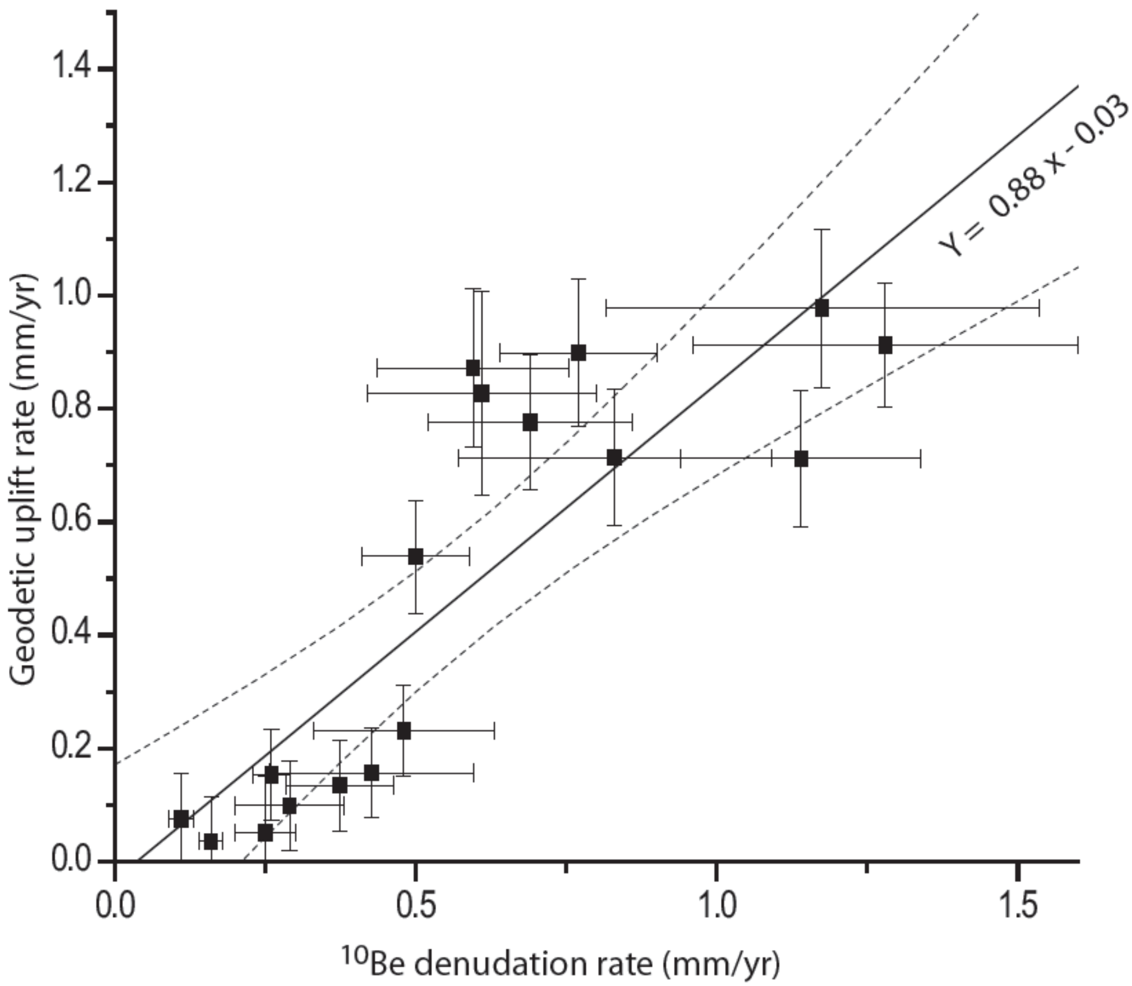

Fig. 5: Denudation rates from cosmogenic ^{10}Be (Wittmann et al., 2008, and Norton et al., 2007) with respect to rock uplift (Schlatter et al. 2005, located at the centroids of each individual watershed measured for cosmogenic nuclides, Fig. 2C). Rock uplift rates for the Anza and Sesia catchments are estimates from interpolated contour lines (Fig 2C) because there are no rock uplift rate measurements in these areas. Rock uplift rate errors of 0.117 mm/yr on the average are the mean errors calculated for survey points within or near a catchment (Schlatter et al., 2005 and personal communication). The errors on the denudation rate data (~5%) include effects from AMS measurements, blank subtraction, and scaling (see Wittmann et al. [2007] and Norton et al. [2008] for details). The linear regression of the data is shown as solid line, and the 95% confidence interval error envelopes as dashed lines. The linear best fit for these data yields a coefficient of correlation of 0.85, a slope of 0.88 ± 0.14 and a vertical axis-intercept of -0.03 ± 0.09.

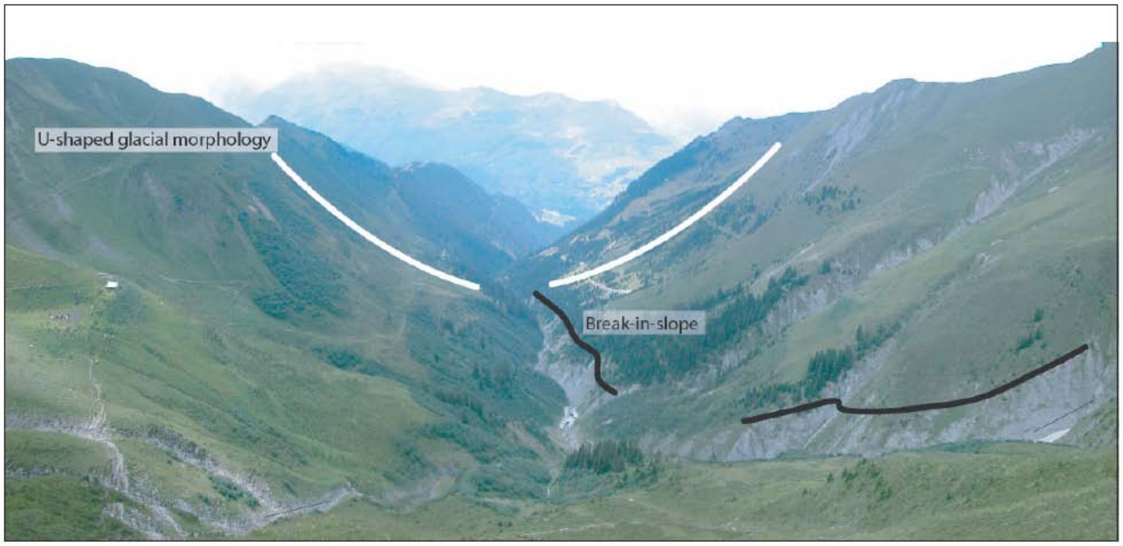

Fig 6: Example illustrating the adjustment of a glacial landscape by modern channelized and associated hillslope processes in the Ilanz area of the Eastern Swiss Alps. The U-shaped morphology dominating this landscape is a relict of glacial processes. Later, Holocene fluvial and associated hillslope processes have resulted in the formation of V-shaped scars in this landscape (beneath the break in slope), which is a strong evidence for ongoing re-adjustment of the Alpine topography to modern climate conditions.

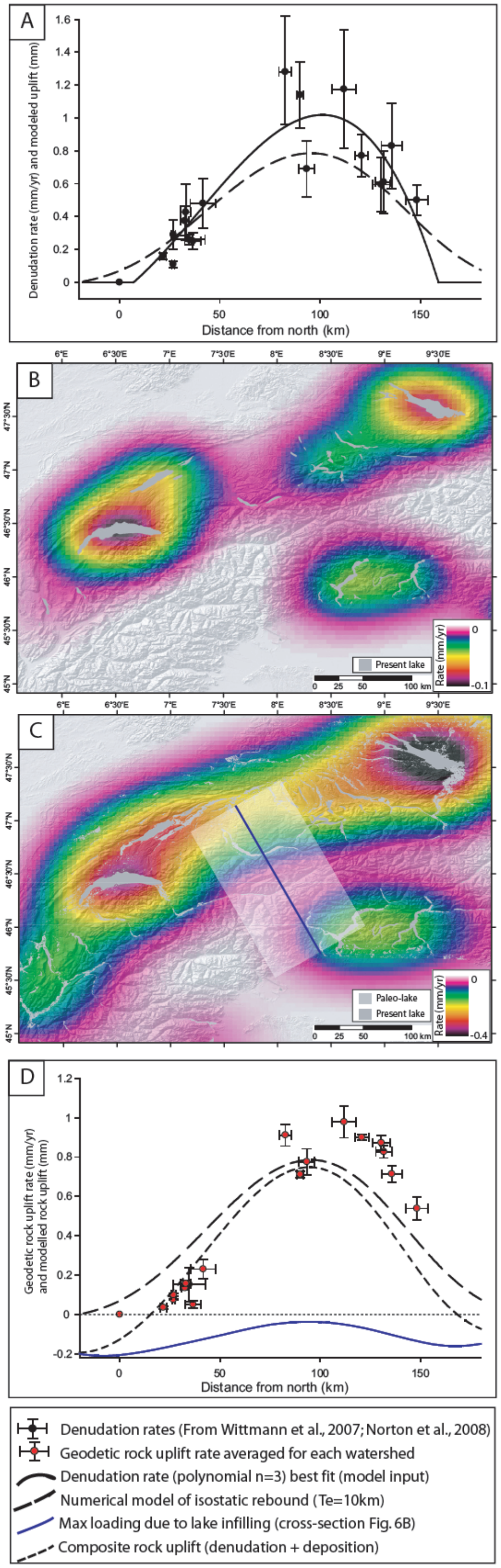
A
Denudation rate (mm/yr) and modeled uplift (mm)
Distance from north (km)
B
Present lake
Rate (mm/yr)
0
-0.1
0 25 50 100 km
C
Paleo-lake
Present lake
Rate (mm/yr)
0
-0.4
0 25 50 100 km
6°E
6°30'E
7°E
7°30'E
8°E
8°30'E
9°E
9°30'E
45°N
45°30'N
46°N
46°30'N
47°N
47°30'N
D
Geodetic rock uplift rate (mm/yr) and modelled rock uplift (mm)
Distance from north (km)
Denudation rates (From Wittmann et al., 2007; Norton et al., 2008)
Geodetic rock uplift rate averaged for each watershed
Denudation rate (polynomial n=3) best fit (model input)
Numerical model of isostatic rebound (Te=10km)
Max loading due to lake infilling (cross-section Fig. 6B)
Composite rock uplift (denudation + deposition)

Fig. 7: (A) Cross section displaying denudation rates of watersheds (black dots) and the associated polynomial (n=3) best fit (set to zero if negative). The dashed line shows a model prediction of lithospheric unloading (rock uplift due to erosion) based on this fit.

(B) Map of the elastic loading due to present sedimentation in the peri-Alpine lakes. See text for details.

(C) Map of the elastic loading due to post-LGM sedimentation in peri-Alpine lakes immediately following deglaciation. Cross section corresponds to the blue line on Fig. 6D. See text for details.

(D) Geodetic rock uplift (red dots) for watersheds in which the denudation rates have been measured (Fig. 2B). The long-dashed line shows the model prediction of lithospheric unloading (rock uplift due to erosion alone) as in Fig 6A. The short-dashed line shows a composite model of both erosional unloading combined with sediment loading in lakes. The blue line is the model prediction of post-LGM sediment loading as shown in Fig 6C. Note that the fit is good in the foreland Basin (left side), but a systematic under prediction is apparent for the southern flank of the belt (right side).